Anisotropy of optical transitions in (110)-oriented quantum wells

S. Nojima
NTT Opto-electronics Laboratories, 3-1 Morinosato-Wakamiya, Atsugi, Kanagawa 243-01, Japan
(Received 31 August 1992)

The in-plane anisotropy of interband optical transitions is theoretically investigated for GaAs/$Al_{0.3}Ga_{0.7}As$ and GaAs/AlAs (110)-oriented quantum-well films. This calculation takes into account the multiplicity of the valence band including the split-off state. The anisotropy analysis reveals that the well-width variation induces an exchange of heavy-hole-like or light-hole-like attributes between the two excited subband states in the valence band. The anisotropy is enhanced to a remarkable degree by narrowing the well, especially in GaAs/AlAs. This theory also clarifies that the pronounced well-width dependence of anisotropy is caused by the presence of the split-off state.

It is now becoming possible to grow semiconductor quantum-well films (QWF's) having growth axes along a variety of crystallographic directions.[1–5] QWF's grown on (110)-oriented substrates are of particular importance,[1,2] because these QWF's have been experimentally shown to exhibit a pronounced in-plane anisotropy in the interband optical transitions. This phenomenon is of great fundamental interest because it reflects the inherent anisotropy of the materials as well as the quantum-confinement states of electronic systems. Optical anisotropy, moreover, reveals the crystallographic directions that generate the most intense optical transitions. This information is very valuable for designing optical devices. Investigating the new crystallographic directions is thus attractive from not only a fundamental point of view but also a technological one. In a previous report,[6] the author clarified some aspects of anisotropy, for an example, by using a simplified QWF model. The entire picture of this phenomenon, however, is not still adequately understood. This paper reports the in-plane anisotropy of (110)-oriented QWF's for a wide range of well widths using a practical model.

We employ the 6×6 Hamiltonian matrix $H_0(k_x',k_y',k_z')$ developed by Kane[7] to describe the valence band in the vicinity of its zone center. This Hamiltonian takes the split-off state into account. Let the above matrix be represented in an O' system with the coordinate axes (x', y', and z') oriented along the cubic axes of the crystal, [100], [010], and [001], respectively. The six bases of the representation are denoted as $X'\alpha'$, $Y'\alpha'$, $Z'\alpha'$, $X'\beta'$, $Y'\beta'$, and $Z'\beta'$. We then rotate the coordinates from the $O'(x',y',z')$ system to an $O(x,y,z)$ system by $\mathbf{r}'=T\mathbf{r}$ where T is the orthogonal transformation characterized by Euler's angles of $(\pi/4,\pi/2,0)$ for (110)-oriented QWF's. The transformation T has been selected so that the new z axis is perpendicular to the QWF interface. Hence, the new x, y, and z axes are oriented along $[00\bar{1}]$, $[\bar{1}10]$, and [110], respectively. Here, note that we do not change the bases of representation of the Hamiltonian matrix. In the framework of effective-mass and envelope function approximations,[8] the wave function of the valence band is written as

$$\Psi^v=S^{-1/2}e^{i\mathbf{k}_{\parallel}\cdot\rho}\mathbf{f}^v(z)\cdot\mathbf{u}^v(\mathbf{r}')\ , \tag{1}$$

where the in-plane envelope function is normalized in the conventional manner [S is the area for this normalization $\mathbf{k}_{\parallel}=(k_x,k_y)$, and $\boldsymbol{\rho}=(x,y)$]. Here, $\mathbf{f}^v(z)$ is a 6×1 column vector, the elements of which are given by the envelope functions in the z direction, and $\mathbf{u}^v(\mathbf{r}')$ is also a 6×1 column vector for base functions ($X'\alpha'$, etc.). The dot ($\cdot$) implies the inner product between the two vectors. The envelope functions are obtained by solving the coupled equation.

$$\{H_0[k_x'(\mathbf{k}_{\parallel},-id_z),k_y'(\mathbf{k}_{\parallel},-id_z),k_z'(\mathbf{k}_{\parallel},-id_z)]+V(z)\}\,\mathbf{f}^v(z)=E\,\mathbf{f}^v(z)\ , \tag{2}$$

where $\mathbf{k}'$ is also transformed by $\mathbf{k}'=T\mathbf{k}$ and k_z is replaced by the operator, $-id_z$ $(=-id/dz)$. Here, $V(z)$ is the 6×6 unit matrix multiplied by the confinement potential $V(z)$ in the z direction. Since H_0 involves terms proportional to k_z and k_z^2, it can be expressed as

$$H_0=R(z)+Q(z)\frac{d}{dz}+P(z)\frac{d^2}{dz^2}\ , \tag{3}$$

where $R(z)$, $Q(z)$, and $P(z)$ are 6×6 matrices which are functions of z through the position-dependent band parameters. This operator is evidently nonHermitian provided that these matrices are z dependent and, therefore it does not give real eigenvalues. To ensure its Hermiticity, Eq. (3) should be interpreted as[9]

$$H_0=R(z)+\tfrac{1}{2}\left[Q(z)\frac{d}{dz}+\frac{d}{dz}Q(z)\right]+\frac{d}{dz}P(z)\frac{d}{dz}\ . \tag{4}$$

Equation (2) is reduced to the matrix eigenvalue problem for the expansion coefficients $\mathbf{a}_n$ when we expand $\mathbf{f}^v(z)$ as

$$\mathbf{f}^v(z)=\sum_n \mathbf{a}_n \phi_n(z) , \tag{5}$$

using an appropriate orthonormal set of functions $\phi_n(z)$. The matrix to be diagonalized possesses the elements consisting of two terms that come from the bulk regions and the heterointerfaces.

The wave function of the conduction band is similarly expressed by

$$\Psi^c = S^{-1/2} e^{i\mathbf{k}_\parallel \cdot \boldsymbol{\rho}} \mathbf{f}^c(z) \cdot \mathbf{u}^c(\mathbf{r}') , \tag{6}$$

where $\mathbf{f}^c(z)$ is a 2×1 column vector, the elements of which are given by the envelope functions in the z direction, and $\mathbf{u}^c(\mathbf{r}')$ is also a 2×1 column vector for base functions ($S'\alpha'$ and $S'\beta'$). Since the two components in $\mathbf{f}^c(z)$ do not couple to each other, the spin-degenerate states are described by $f^c(z)$ which possesses the identical function as its component.

The optical transition matrix elements between Ψ^c and Ψ^v is written as

$$M_{cv} = \langle \Psi^c | \boldsymbol{\varepsilon}' \cdot \mathbf{p}' | \Psi^v \rangle , \tag{7}$$

where $\boldsymbol{\varepsilon}'$ is the unit vector denoting the direction of the polarization of the light and $\mathbf{p}'$ is the momentum operator. Here, we represented $\boldsymbol{\varepsilon}'$ and $\mathbf{p}'$ in the O' system, since it is easier to find the momentum matrix element between $\mathbf{u}^c(\mathbf{r}')$ and $\mathbf{u}^v(\mathbf{r}')$ in the O' system than in the O system; for example, we can easily obtain relations such as $\langle S' | p_x' | Y' \rangle = 0$. It may be more convenient, however, to describe the final results using the direction $\boldsymbol{\varepsilon}$ of the polarization vector represented in the O system. Using the transformation $\boldsymbol{\varepsilon}' = T\boldsymbol{\varepsilon}$, we obtain the squared momentum matrix element (SMME),

$$|M_{cv}|^2 = |\mathbf{c}\cdot\boldsymbol{\varepsilon}|^2 M^2 , \tag{8}$$

where $M = \langle S' | p_x' | X' \rangle$ is a momentum matrix element[10] and $\mathbf{c}$ is a constant vector which is, however, a function of the material, the well width, and the transition concerned. When we consider the transition between the μth subband in the conduction band and the νth subband in the valence band, these two subband states are doubly degenerate. Here, we distinguish these degenerate states by denoting ($\Psi^c_{+\mu}$ and $\Psi^c_{-\mu}$) and ($\Psi^v_{+\nu}$ and $\Psi^v_{-\nu}$). The so-called μ-ν optical transition is the sum of four possible transitions between these states: $\Psi^c_{+\mu}-\Psi^v_{+\nu}$, $\Psi^c_{-\mu}-\Psi^v_{-\nu}$, $\Psi^c_{+\mu}-\Psi^v_{-\nu}$, and $\Psi^c_{-\mu}-\Psi^v_{+\nu}$. At the zone center, the first two transitions give the identical matrix element value as do the next two. Let us denote the sum of the first two SMME's as $2|M_{cv}|^2_{+(\mu,\nu)}$ and the next two as $2|M_{cv}|^2_{-(\mu,\nu)}$. The total sum

$$|M_{cv}|^2_{\mu,\nu} = 2(|M_{cv}|^2_{+(\mu,\nu)} + |M_{cv}|^2_{-(\mu,\nu)}) \tag{9}$$

is the SMME which is observable for the μ-ν transition at the zone center.

We applied the above formulation to two kinds of (110)-oriented QWF's, GaAs/$Al_{0.3}Ga_{0.7}As$ and GaAs/AlAs. Let us consider a symmetrical QWF (well layer is in $d<z<d+L$ and barrier layers are in $0<z<d$ and $d+L<z<2d+L$, where L is the well width). In these practical calculations, we used sinusoidal waves for $\phi_n(z)$ defined in the range $0<z<R$ ($R=2d+L$). The range $0<z<R$ must cover the extension of the actual wave functions (so, d should be large); but an unnecessarily large d would complicate the convergence of the series [Eq. (5)]. The choice of d is thus critical for the numerical analysis. We selected a value of d that is 5 to 30 times the extension estimated at the zone center ($\mathbf{k}_\parallel=\mathbf{0}$) for the light-hole ground-state wave function. This value adequately covers the extension of the heavy-hole state since the latter is more localized than the former. The valence-band parameters used in our calculations are the following: $A=17.3$, $B=2.83$, $C=19.7$, and $\Delta=340$ meV for GaAs; $A=14.3$, $B=2.73$, $C=16.6$, and $\Delta=322$ meV for $Al_{0.3}Ga_{0.7}As$; $A=7.16$, $B=2.48$, $C=9.42$, and $\Delta=280$ meV for AlAs in the usual notations.[10] The electron effective masses for these materials are $0.067m_0$, $0.11m_0$, and $0.22m_0$, respectively. The offsets of the valence band and the conduction band are selected as 125 and 249 meV, respectively, for the former QWF, and those for the latter are 417 and 830 meV.

Figure 1 shows (a) the index of the in-plane anisotropy defined by

$$\Gamma = \frac{|M_{[\bar{1}10]}|^2}{|M_{[00\bar{1}]}|^2} \tag{10}$$

for several kinds of optical transitions, and (b) the subband energy in the valence band (upper part) as a function of the well width L of GaAs/$Al_{0.3}Ga_{0.7}As$ (110) QWF's. The lower part of Fig. 1(b) will be explained later. Here, $M_{[00\bar{1}]}$ and $M_{[\bar{1}10]}$ are the zone-center ($\mathbf{k}_\parallel=\mathbf{0}$) optical transition matrix elements [Eq. (9)] for the light polarized in $x\,[00\bar{1}]$ [i.e., $\boldsymbol{\varepsilon}=(1,0,0)$] and $y\,[\bar{1}10]$ [i.e., $\boldsymbol{\varepsilon}=(0,1,0)$] directions, respectively. We focus on the above zone-center matrix elements because they determine the most important properties relating to interband optical transitions. The optical transition between the μth subband in the conduction band ($C\mu$) and the νth subband in the valence band ($V\nu$) is denoted by $C\mu$-$V\nu$ in Fig. 1 (for $\mu=0,1$ and $\nu=0,1,2,3$). Transitions indicated by the dashed-dotted lines are much weaker than those indicated by the solid lines. The subband states in the valence band are an admixture of the heavy-hole, light-hole, and split-off states even at $k_\parallel=0$ for the QWF of this orientation. We then introduce the symbols $\tilde{H}n$ and $\tilde{L}n$ ($n=0,1,2$) to indicate heavy-hole-like and light-hole-like characteristics, respectively. Here, $\tilde{H}n$ implies that the amplitude of the heavy-hole state is dominant compared with those for the light-hole and split-off states; $\tilde{L}n$ implies that the light-hole state is dominant in a similar manner. The in-plane anisotropy of optical transitions is manifested in the deviation of Γ from unity.

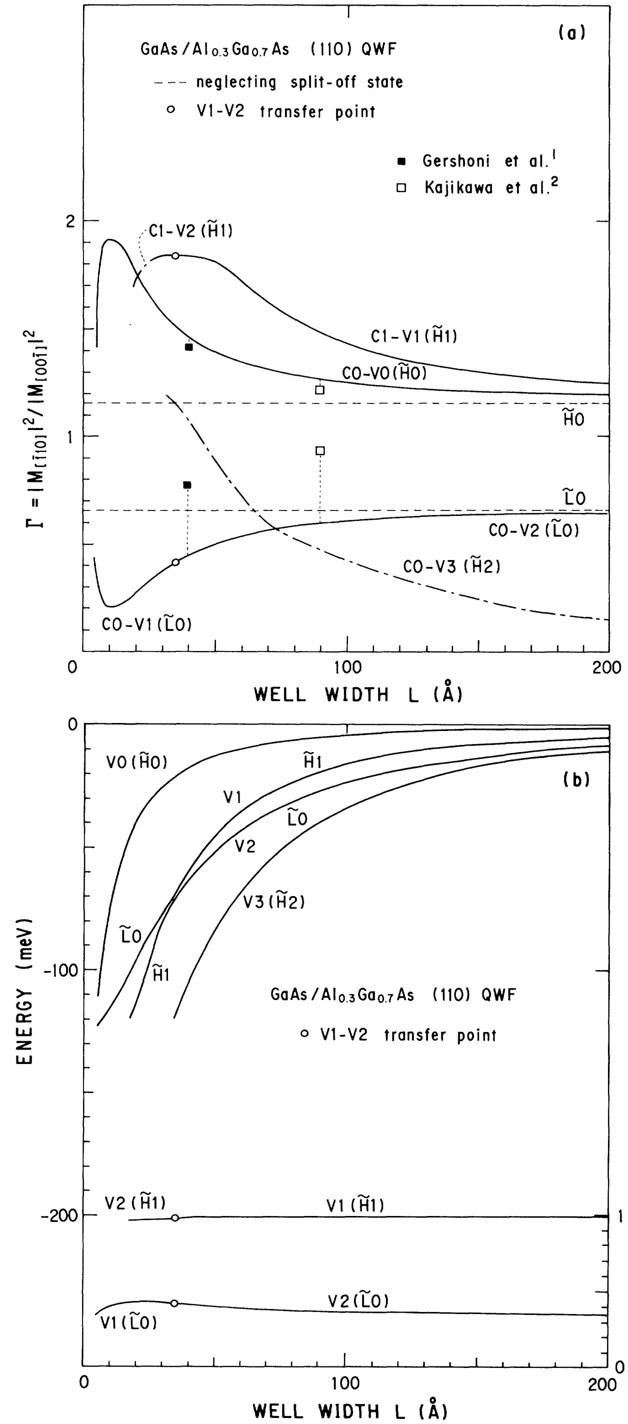

FIG. 1. (a) Index of the in-plane anisotropy Γ and (b) subband energy levels in the valence band (upper) and measure of heavy-hole mixing χ_H (lower) as a function of well width L for GaAs/$Al_{0.3}Ga_{0.7}As$ (110)-oriented quantum-well films for several optical transitions (denoted by $C\mu$-$V\nu$). Γ is defined by the ratio between the transition matrix elements at the zone center [(Eq. (10)]. $C\mu$ and $V\nu$ indicate the subband states in the conduction and valence bands, respectively. Transitions indicated by the dashed-dotted lines are much weaker than those indicated by solid lines. Circles mark the point ($L \sim L_c$) where the $V1$ and $V2$ states exchange their attributes.

The ground-state $V0$ couples to the ground-state $C0$ in the conduction band and produces the band-edge transition $C0$-$V0(\tilde{H}0)$. The Γ value for this transition increases as L decreases and, after reaching a maximum value of 1.9, it decreases rapidly. This is caused by a wave function overflowing out of the well by narrowing the QWF. The first excited state $V1$ reveals odd behavior. There seems to be a critical well width L_c around 35 Å (as indicated by circles in Fig. 1). For $L < L_c$, $V1$ appears to have the light-hold character ($\tilde{L}0$) and therefore couples to $C0$. For $L > L_c$, however, it behaves as a heavy-hole-like state ($\tilde{H}1$) and couples to $C1$. The second excited state $V2$ exhibits behavior that is complementary to that of the $V1$ state. Namely, the $V2$ state possesses the $\tilde{H}1$ character producing the weak $C1$-$V2$ transition for $L < L_c$, while it shows the $\tilde{L}0$ character producing the $C0$-$V2$ transition for $L > L_c$. Despite the abrupt change, the anisotropy index for the $C0$-$\tilde{L}0$ and $C1$-$\tilde{H}1$ transitions exhibits a smooth continuum in the vicinity of this transfer point. This phenomenon can be understood in terms of increased interaction between the two ($V1$ and $V2$) states due to their close energy levels. We consider this in more detail below.

Let us define an index χ_H representing heavy-hole mixing in the subband states. First, we consider a (001)-oriented QWF, in which the heavy-hole state does not couple to either light-hole or split-off states at the zone center. In other words, this QWF exhibits a pure heavy-hole state. The heavy-hole state is characterized by the absence of a z [001] component in the SMME ($|M_z|^2=0$). Hence, the index defined by

$$\chi_H = 1 - \frac{|M_z|^2}{|M_T|^2} \tag{11}$$

can be regarded as a measure of heavy-hole mixing in the coupled subband states. Here, $|M_T|^2=|M_x|^2+|M_y|^2+|M_z|^2$ is the total sum for the SMME in all directions, and x, y, and z indicate the [100], [010], and [001] directions, respectively, for (001) QWF's. By this definition, the pure heavy-hole state is evidently described by $\chi_H=1$. Moreover, it is easy to show that the pure light-hole state and the pure split-off state are characterized by $\chi_H=\frac{1}{3}$ and $\chi_H=\frac{2}{3}$, respectively. This index can be extended to QWF's having any growth axes—(110) QWF's, for example—if we regard x, y, and z directions as $[00\bar{1}]$, $[\bar{1}10]$, and [110], respectively. In the lower part of Fig. 1(b), χ_H for $V1$ and $V2$ states is depicted as a function of L. The $V1$ ($V2$) state for $L < L_c$ and the $V2$ ($V1$) state for $L > L_c$ are assigned to $\tilde{L}0$ ($\tilde{H}1$) rather than $\tilde{H}1$ ($\tilde{L}0$), since these states possess χ_H values close to the value of the pure light-hole (heavy-hole) state $\frac{1}{3}$ (1). The abrupt transfer of their attributes can be understood by examining the subband energy diagram [the upper part of Fig. 1(b)]. Note that $V1$ and $V2$ states have the closest energy in the vicinity of L_c. This is induced

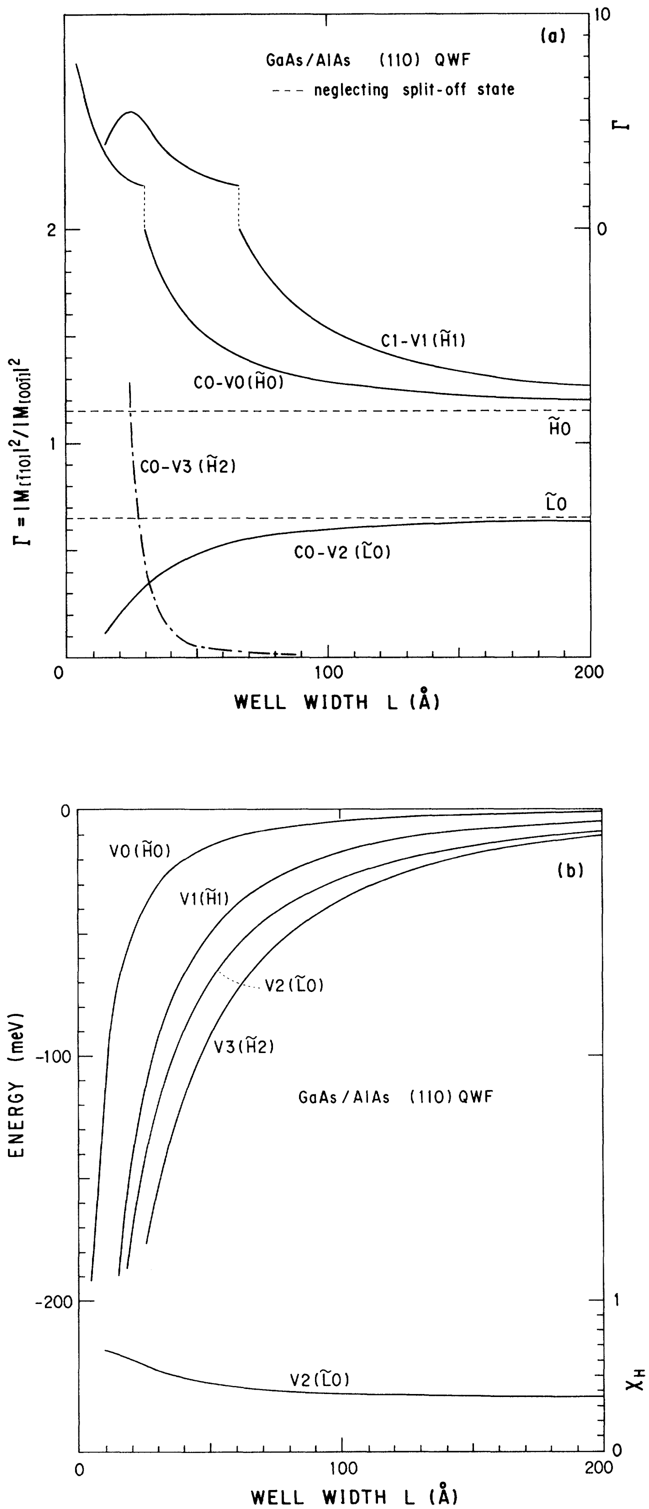

FIG. 2. (a) Index of the in-plane anisotropy Γ and (b) subband energy levels in the valence band (upper) and measure of heavy-hole mixing χ_H (lower) as a function of well width L for GaAs/AlAs (110)-oriented quantum-well films. Other details are given in the caption of Fig. 1.

by the two energy levels approaching and then moving apart due to the repulsion between them (anticrossing). At the transfer point (i.e., $L \sim L_c$), one state exchanges its attribute for that of another. Other states such as $V0$ and $V3$ do not exhibit this phenomenon, because they are remote from the neighboring levels throughout the well width studied here. Figure 1(a) also shows the experimental results obtained by Gershoni *et al.*[1] using photoluminescence excitation spectroscopy and Kajikawa *et al.*[2] using photocurrent spectroscopy for $\tilde{H}0$ and $\tilde{L}0$ states. Good agreement is obtained between theoretical and experimental results, especially for the $C0$-$V0(\tilde{H}0)$ transition.

Results for GaAs/AlAs (110) QWF's are presented in a similar manner in Fig. 2. In this QWF, the transfer of the light-hole ($\tilde{L}0$) attribute does not occur owing to the pronounced energy separation between the states. The $V2$ state thus possesses the character of $\tilde{L}0$ throughout the well width studied here, except for the very small L region where it appears to exhibit the beginning of a transfer. Note that the anisotropy for the $C0$-$V0(\tilde{H}0)$ transition is enhanced to a remarkable degree by narrowing the well, and it approaches a value as high as about 8. The large potential barrier at the hetero-interfaces for this QWF may prevent the wave-function overflow and resultant attentuation of the anisotropy. In fact, we estimate the Γ value at 1.55 for $L = 50$ Å, which is close to the value (1.63) derived for the QWF with infinitely deep potential barrier.[6]

Our theory has clarified the pronounced well-width dependence of in-plane anisotropy. Earlier published reports[11,12] do not describe this well-width dependence [see the broken lines for $\tilde{H}0$ and $\tilde{L}0$ in Figs. 1(a) and 2(a)]. The reason is that their calculations have neglected the split-off state and described the valence band using the 4×4 Hamiltonian. It is easy to show that such a simplification makes the eigenvectors $\mathbf{a}_n$ in Eq. (5) independent of the well width, while our theory does not. As a result, the in-plane anisotropy Γ becomes constant throughout the well width in their simplified calculations. The split-off state in the valence band is thus known to play an important role in the analysis of optical anisotropy. As shown in Figs. 1(a) and 2(a), our anisotropy index tends to converge with their index for larger well widths. This is more easily explained by considering a QWF with an infinitely deep potential barrier and using a 6×6 Luttinger matrix[8] rather than the 6×6 Kane matrix[7] employed in this paper (the two matrices differ only in their representations). Since the ground-state envelope function has the form of $\sin(\pi z/L)$, the Luttinger matrix for the ground subband state at the zone center is described by the sum of two matrices: the matrix consisting of elements which are proportional to L^{-2}, and the matrix possessing nonzero diagonal elements Δ only in the lower right 2×2 submatrix. In the limit of either large L or large Δ, the seqular equation for the 6×6 matrix decouples into determinants for the 4×4 and 2×2 submatrices, the former of which corresponds to the approximation neglecting the split-off state. The larger well width is thus known to be equivalent to the larger spin-orbit splitting, which permits one to neglect the split-off state.

[1]D. Gershoni, I. Brener, G. A. Baraff, S. N. G. Chu, L. N. Pfeiffer, and K. West, Phys. Rev. B **44**, 1930 (1991).

[2]Y. Kajikawa, M. Hata, T. Isu, and Y. Katayama, Surf. Sci. **267**, 501 (1992).

[3]T. Hayakawa, K. Takahashi, M. Kondo, T. Suyama, S. Yamamoto, and T. Hijikata, Phys. Rev. Lett. **60**, 349 (1988).

[4]L. W. Molenkamp. R. Eppenga, G. W. 't Hooft, P. Dawson, C. T. Foxon, and K. J. Moore, Phys. Rev. B **38**, 4314 (1988).

[5]B. W. Shanabrook, O. J. Glembocki, D. A. Broido, and W. I. Wang, Phys. Rev. B **39**, 3411 (1989).

[6]S. Nojima, Jpn. J. Appl. Phys. **31**, L765 (1992).

[7]E. O. Kane, J. Phys. Chem. Solids **1**, 82 (1956).

[8]J. M. Luttinger and W. Kohn, Phys. Rev. **97**, 869 (1955).

[9]S. Nojima, Jpn. J. Appl. Phys. **31**, L1401 (1992).

[10]P. Lawaetz, Phys. Rev. B **4**, 3460 (1971).

[11]G. E. W. Bauer, in *Spectroscopy of Semiconductor Microstructures,* edited by G. Fasol, A. Fasolino, and P. Lugli (Plenum, New York, 1989), p. 381.

[12]Y. Kajikawa, M. Hata, and T. Isu, Jpn. J. Appl. Phys. **30**, 1944 (1991).